5366579

Cloud Overlapping Detection Algorithm Using Solar And IR Wavelengths With GOES Data Over ARM/SGP Site

Kazuaki Kawamoto[1], Patrick Minnis[2] and William L. Smith, Jr.[2]

[1] Virginia Polytechnic Institute and State University
[2] NASA Langley Research Center

k.kawamoto@larc.nasa.gov
757-864-5673

Abstract
Proceedings of 11th ARM Science Team Meeting
Atlanta, Georgia
March 19-23, 2001

Cloud Overlapping Detection Algorithm Using Solar And IR Wavelengths With GOES Data Over ARM/SGP Site

Kazuaki Kawamoto[1], Patrick Minnis[2] and William L. Smith, Jr.[2]

[1] Virginia Polytechnic Institute and State University
[2] NASA Langley Research Center

k.kawamoto@larc.nasa.gov
757-864-5673

Introduction

One of the most perplexing problems in satellite cloud remote sensing is the overlapping of cloud layers. Although most techniques assume a 1-layer cloud system in a given retrieval of cloud properties, many observations are affected by radiation from more than one cloud layer. As such, cloud overlap can cause errors in the retrieval of many properties including cloud height, optical depth, phase, and particle size. A variety of methods have been developed to identify overlapped clouds in a given satellite imager pixel. *Baum et al. (1995)* used CO_2 slicing and a spatial coherence method to demonstrate a possible analysis method for nighttime detection of multilayered clouds. *Jin and Rossow (1997)* also used a multispectral CO_2 slicing technique for a global analysis of overlapped cloud amount. *Lin et al. (1999)* used a combination infrared, visible, and microwave data to detect overlapped clouds over water. Recently, *Baum and Spinhirne (2000)* proposed 1.6 and 11 μm bispectral threshold method. While all of these methods have made progress in solving this stubborn problem, none have yet proven satisfactory for continuous and consistent monitoring of multilayer cloud systems. It is clear that detection of overlapping clouds from passive instruments such as satellite radiometers is in an immature stage of development and requires additional research. Overlapped cloud systems also affect the retrievals of cloud properties over the ARM domains (e.g., *Minnis et al. 1998*) and hence should identified as accurately as possible. To reach this goal, it is necessary to determine which information can be exploited for detecting multilayered clouds from operational meteorological satellite data used by ARM. This paper examines the potential information available in spectral data available on the Geostationary Operational Environmental Satellite (GOES) imager and the NOAA Advanced Very High Resolution Radiometer (AVHRR) used over the ARM SGP and NSA sites to study the capability of detecting overlapping clouds.

Data

This study uses daytime half-hourly GOES-8 4-km data from channels 1, 2, 4, and 5, at visible (VIS; 0.65 μm), solar-infrared (SI; 3.9 μm), infrared (IR; 10.8 μm), and split-window (WS; 12.0 μm) wavelengths, respectively, and the cloud properties over the ARM SGP central facility (SCF) derived from these radiances by *Minnis et al. (2001)* for all of 1998. The ARM 35-GHz radar data taken over the SCF are used to provide cloud boundary data to determine the presence of single and multilayered clouds during each 10-minute period centered on a given GOES image time. The average GOES

radiances and cloud properties for a 0.3° box centered on the SCF are compared to the cloud boundary data from the corresponding radar data.

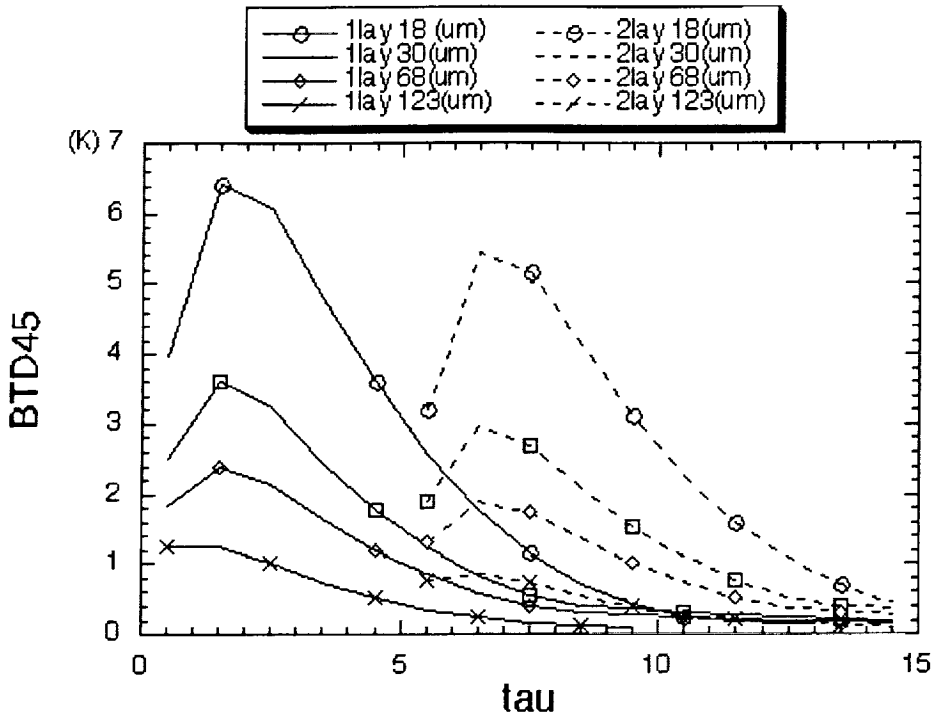

Fig. 1. Theoretical brightness temperature differences for one and two layer cloud systems.

Methods and Results

Two methods for detecting multilayered clouds are proposed. The first one relies on the brightness temperature difference between channels 4 and 5 (hereafter BTD_{45}). The basic assumption for this approach is that for large cloud optical depth τ, BTD_{45} should be small, nearly equal to zero, if the cloud is a single layer because the emissivities in both channels approach unity. On the other hand, if BTD45 is large and τ is large, a thin cloud probably overlaps a lower cloud. Thus, BTD_{45} should be an indicator of overlapping clouds when the τ is large. To illustrate this situation, Fig. 1 shows the results of a numerical simulation using the parameterizations of *Minnis et al. (1998)*. The values of BTD_{45} are plotted as functions of total optical depth OD and effective cloud particle size for single and 2-layer cases. The single cloud is ice layer with OD between 0.5 and 9.5 with an effective diameter D_e = 18, 30, 68 and 123 μm. The 2-layer system consists of a low cloud τ = 10 and an effective droplet radius r_e = 10 μm overlaid by the high cloud used in the single-layer case. Cloud-top temperatures of 245 K and 275 K are used for the high and low clouds, respectively. The figure demonstrates that the values of BTD_{45} for the 2-layer cloud system are greater than their single-layered counterparts for a given value of total OD. In this case, values of BTD_{45} exceeding about 0.6K for $\tau > 8$ should indicate the presence of multilayered clouds. Although a great variety of cloud temperature, optical depth, and particle size combinations will occur, BTD_{45} values should follow a pattern similar to that in Fig. 1.

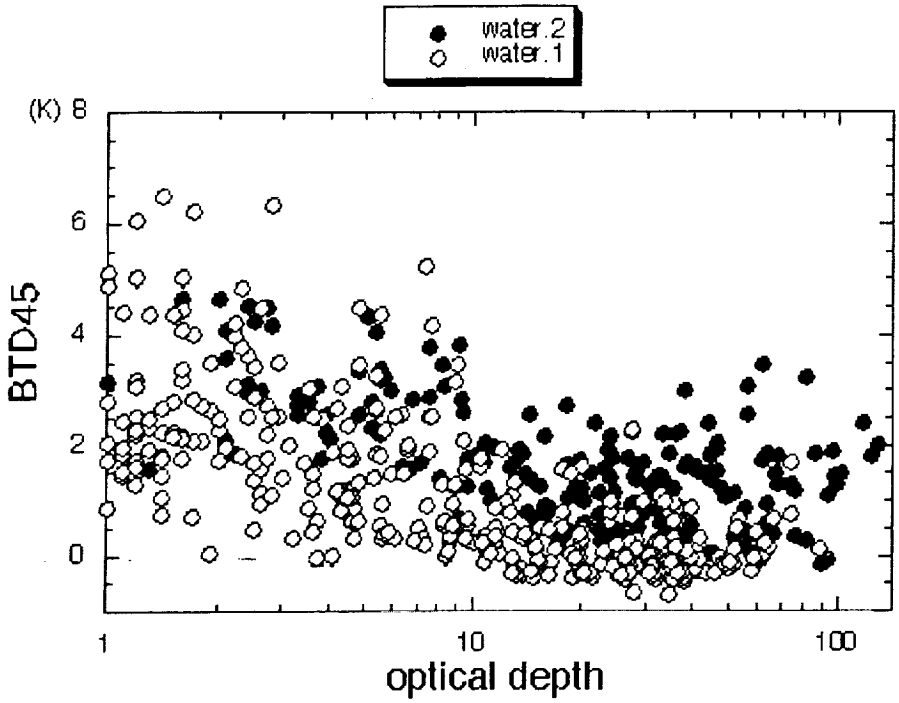

Fig. 2. Brightness temperature differences for single and multilayered clouds over the SCF identified as liquid phase only from GOES-8.

Figures 2 and 3 plot the observed BTD_{45} values as a function of the retrieved OD for both single and multilayered clouds having $BTD_{45} > 0.5$ K and $\tau > 10$ correspond to multilayered clouds. For smaller BTDs, only 21% of the clouds are multilayered. If a BTD45 of 1 K is used as the threshold, 85% of the clouds are multilayered for larger BTD_{45}, but 28% of the multilayered clouds would be identified as single-layered. At lower optical depths, BTD_{45} is generally greater than that from the single-layer clouds, but no clear threshold values are evident for selecting single versus multilayered clouds. For clouds identified as ice (Fig. 3), only 60% of the pixels are clearly multilayered using a threshold of $BTD_{45} = 0.5$ K for the optically thick clouds. Many of the optically thicker clouds have $BTD_{45} > 1.0$ K. If the threshold of 1.0 K is used for the ice clouds, 82% of the clouds with larger BTD_{45} are multilayered and 36% of the clouds with smaller BTD_{45} are single layered. The differences between Figs. 2 and 3 may be due to the low density of ice clouds and their infrared scattering properties. Because the phase discrimination is based on models of cloud particle sizes, the ice cloud emissions probably dominate the clouds identified as ice, while those determined to be water most likely have only a thin layer of ice cloud over the low-level water cloud. The water clouds are generally dense so the radiating temperatures for both channels in the single-layer case are probably very close. Optically thin ice clouds can be several kilometers thick with vertically dependent microphysical properties. Optically thicker ice clouds also may be very thick physically with a layer of low-density cirrus at the top of the cloud. These low-density clouds or cloud layers could easily produce $BTD_{45} = 1$ K, even for optically thick clouds because of their vertical structure. Thus, detecting mulitlayering for clouds identified as ice is more difficult than for water clouds using this approach. The second method uses particle size for detecting overlapping clouds. The method applied by *Minnis et al. (2001)* assumes that the observed cloud in a given imager pixel is a single-layered cloud and uses the 3.7 and 11-μm brightness temperature difference BTD_{34} to determine phase and effective particle size. For a given value of τ, BTD_{34} is smallest for large ice crystals and greatest for small droplets. From the smallest water droplet radius,

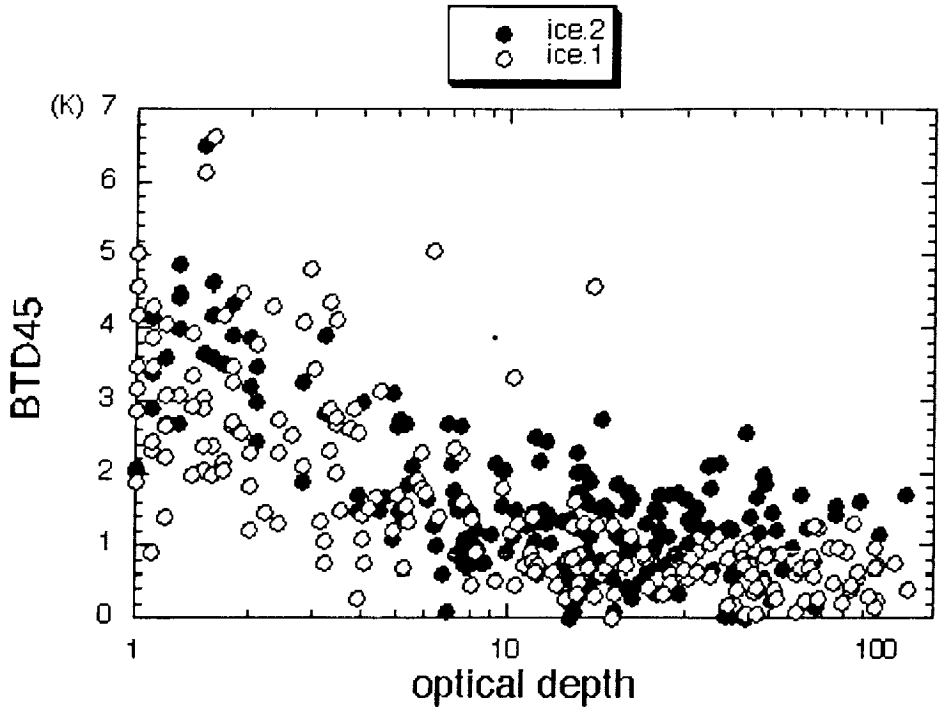

Fig. 3. Same as Fig. 2, except for clouds identified as ice phase only.

droplet size generally increases as BTD_{34} decreases. Conversely, starting with the largest ice crystal, D_e decreases as BTD_{34} increases. The value of BTD_{34} may correspond to both large water droplets and small ice crystals for intermediate cases. Thus, if a relatively thin ice cloud overlaps a water cloud, the retrieved value of r_e or D_e may be either very large or extremely small, respectively, depending on the optical depth of the upper level cloud. Motivated by this idea, effective particle sizes were plotted against the retrieved OD values for single and multilayered cases as determined by the 35-GHz cloud radar. Figures 4 and 5 show scatter plots for the water and ice cases, respectively. For larger ODs, very few single-layer clouds occur with $r_e > 15$ μm. However, some multilayered clouds have smaller droplet radii. Both large and small droplet sizes occur for the smaller ODs with no clear distinction between the single- and multilayered clouds. Pixels that are only partially cloud filled could be responsible for the larger values of r_e at small ODs. In the ice case, the multilayer clouds generally correspond to $D_e < 70$ μm for $\tau > 6$. At smaller ODs, large and small ice crystals occur for both single and multilayered systems. Histograms of the particle sizes for $\tau > 10$ are shown in Figs. 6 and 7. As noted before, the largest droplets (Fig. 6) correspond primarily to overlapped clouds, but many of the multilayer systems yield values of r_e that are within the observed probability distribution for single-layer clouds. Better discrimination may be possible for the ice clouds because the single and multilayered D_e histograms are substantially different with peaks at 50 and 80 μm, respectively. Using a threshold of $D_e = 70$ μm would identify 84% of the multilayered clouds having a total OD greater than 8. However, it would misidentify 23% of the single-layered clouds having relatively small ice particle sizes thus skewing the ice crystal size distribution. By combining both methods, it may be possible to account for some of the weaknesses in the two techniques used alone. For example, the BTD_{45} data provide minimal discrimination for overlapped clouds identified as ice, but the particle size can be used to detect many of the overlapped ice clouds. Conversely, the particle size is not particularly helpful in the identification of many overlapped water clouds, but BTD_{45} appears to be useful in this case.

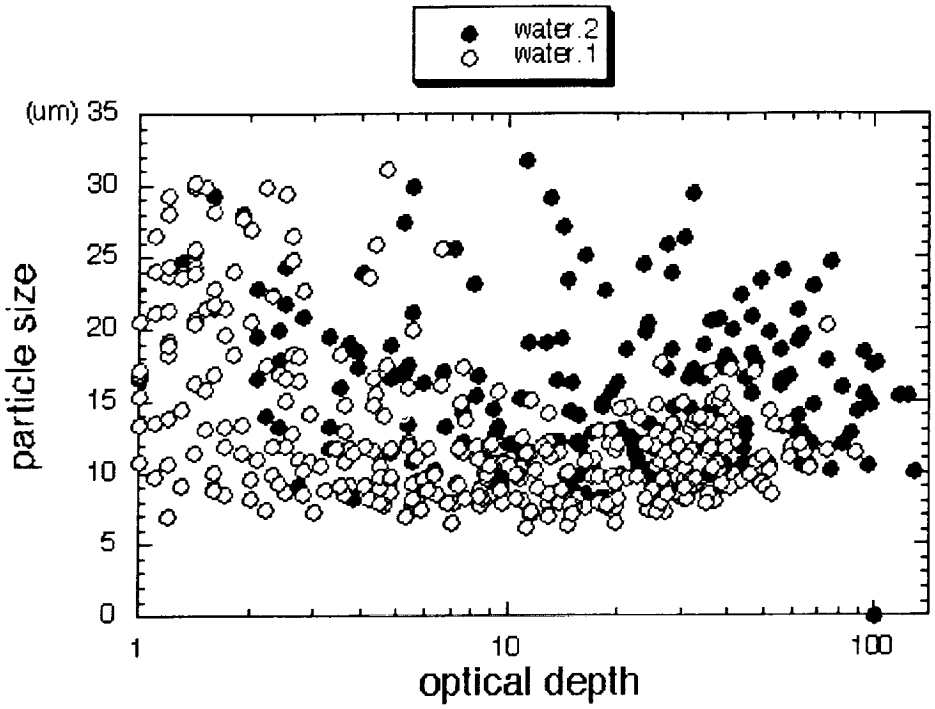

Fig. 4. Effective droplet radius for single and multilayered liquid phase clouds from GOES-8.

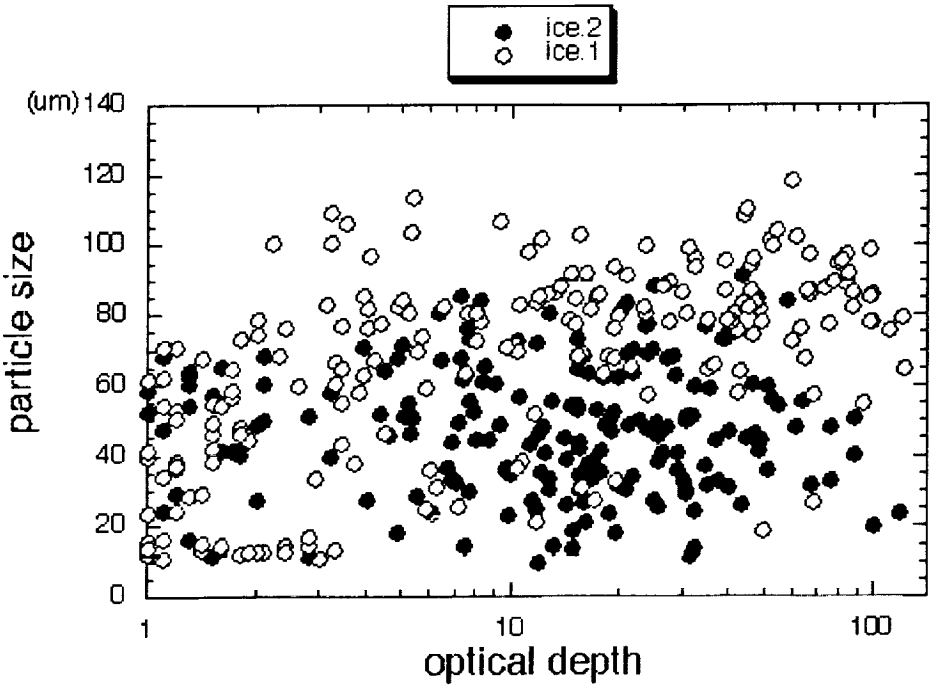

Fig. 5. Same as Fig. 4, except for ice phase only.

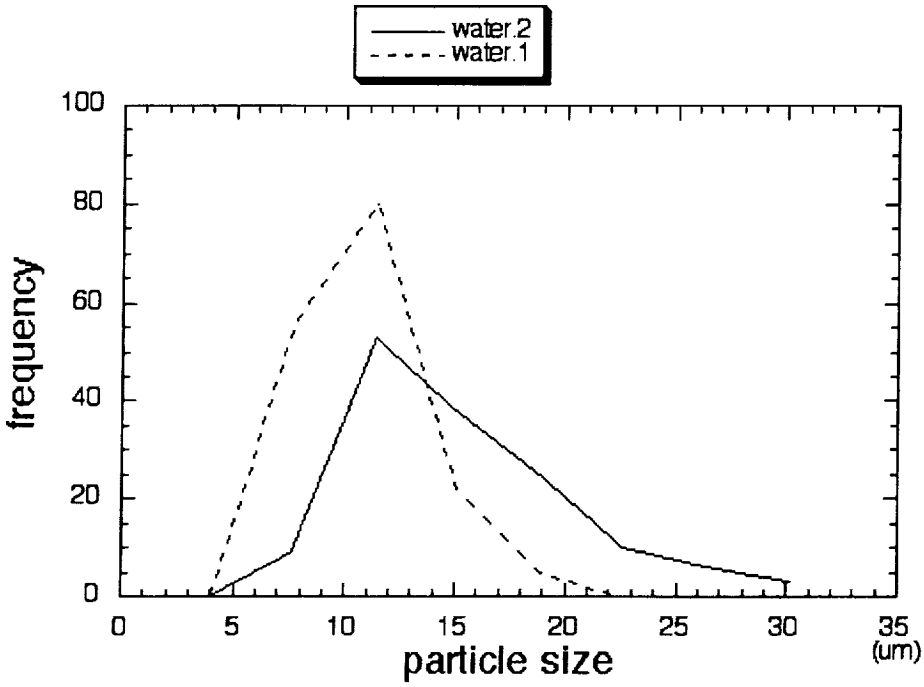

Fig. 6. Histograms of cloud water droplet radius for single and multilayered clouds.

Discussion and concluding remarks

The results found here indicate that a multilayered detection algorithm using BTD45 with the derived phase and particle sizes may provide accuracies of ~80% for cloud systems having optical depths greater than 8 to 10. Detection of multilayered systems with smaller ODs or with better accuracy requires much additional study. The radar cloud multilayering classification used a broad definition of cloud overlap. Precipitating clouds, broken clouds, and water-over-water and ice-over-ice clouds were included in the dataset. The amount of cloud layer separation was not specified, so that two layers only several hundred meters apart may have been included. By further subsetting the dataset using this additional information, it should be possible to refine the criteria needed to determine the presence of multilevel clouds. It will also be possible to define the conditions when this method is applicable.

This paper is the first step in developing a robust method for detecting multilayered clouds using the satellite imager channels available for the most routine monitoring of clouds over the ARM sites. Further study will be devoted to examining the impact of cloud temperature, fraction, and layer gaps on the thresholds that could be used for identifying multilayered clouds. By gathering similar datasets over the NSA and TWP sites, it should be possible to adjust any algorithm for the particular environment.

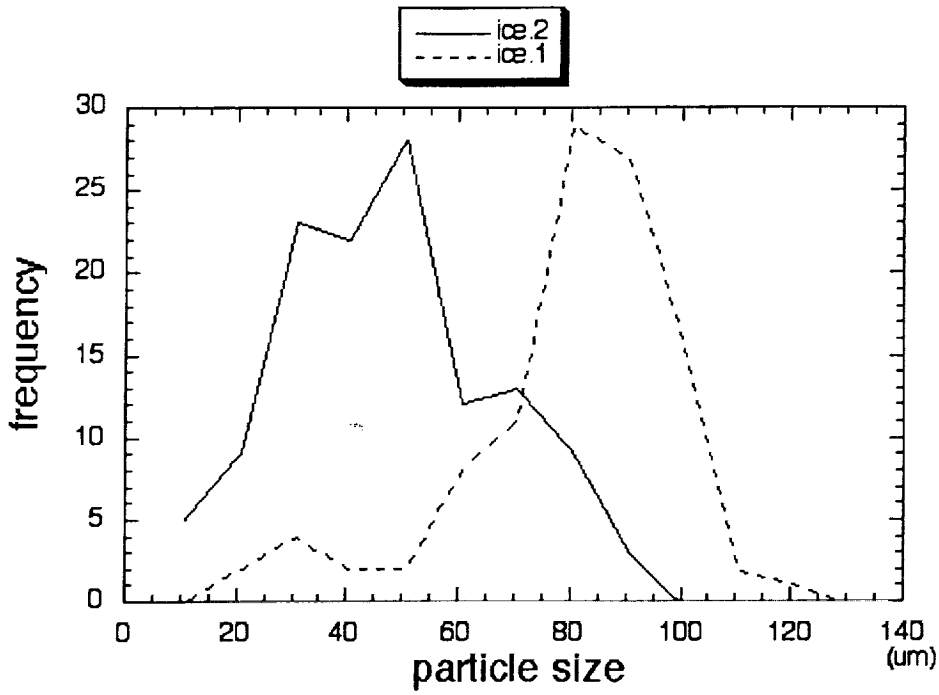

Fig. 7. Same as Fig. 6, except for cloud ice crystal diameter.

Acknowledgments

The authors are grateful to Seiji Kato for helping radar data processing and Robert Arduini for supplying radiative transfer calculation results.

References

Baum, B. A., J. M. Alvarez, T. Uttal, J. Intrieri, M. Poellot, E. Clothiaux, T. P. Ackerman, D. O'C. Starr, J. Titlow and V. Tovinkere, 1995: Satellite remote sensing of multiple cloud layers. *J. Atmos. Sci.*, **52**, 4210–4230.

Baum. B. A. and J. D. Spinhirne, 2000: Remote sensing of cloud properties using MODIS airborne simulator imagery using SUCCESS, 3: cloud overlap. *J. Geophys. Res.*, **105**, 11793-11801, 2000.
Jin, Y. and W. B. Rossow, 1997: Detection of cirrus overlapping low-level clouds. *J. Geophys. Res.*, **102**, 1727-1737.

Jin, Y. and W. B. Rossow, 1997: Detection of cirrus overlapping low-level clouds. *J. Geophys. Res.*, **102**, 1727-1737.

Lin, B., P. Minnis, B. A. Wielicki, D. R. Doelling, R. Palikonda, D. F. Young, and T. Uttal, 1998: Estimation of water cloud properties from satellite microwave and optical measurements in oceanic environments. II: Results. *J. Geophys. Res.*, **103**, 3887-3905.

Minnis, P., D. P. Garber, D. F. Young, R. F. Arduini and Y. Takano, 1998: Parameterizations of reflectance and effective emittance for satellite remote sensing of cloud properties. *J. Atmos. Sci.*, **55**, 3313–3339.

Minnis, P., W. L. smith, Jr., and D. F. Young, 2001: Cloud macro- and microphysical properties derived from GOES over the ARM SGP domain. *Proc. ARM 11th Science Team Meeting*, Atlanta, GA, March 19-23.